Constraints on determining the eruption style and composition of terrestrial lavas from space

Robert Wright[1]*, Lori Glaze[2], and Stephen M. Baloga[3]

[1]Hawai'i Institute of Geophysics and Planetology, University of Hawai'i at Mānoa, Honolulu, Hawaii 96822, USA
[2]National Aeronautics and Space Administration, Goddard Space Flight Center, Greenbelt, Maryland 20771, USA
[3]Proxemy Research Inc., 20528 Farcroft Lane, Gaithersberg, Maryland 20882, USA

ABSTRACT

The surface temperatures of active lavas relate to cooling rates, chemistry, and eruption style. We analyzed 61 hyperspectral satellite images acquired by the National Aeronautics and Space Administration's Earth Observing–1 (EO-1) Hyperion imaging spectrometer to document the surface temperature distributions of active lavas erupted at 13 volcanoes. Images were selected to encompass the range of common lava eruption styles, specifically, lava fountains, flows, lakes, and domes. Our results reveal temperature distributions for terrestrial lavas that correlate with composition (i.e., a statistically significant difference in the highest temperatures retrieved for mafic lavas and intermediate and felsic lavas) and eruption style. Maximum temperatures observed for mafic lavas are ~200 °C higher than for intermediate and felsic lavas. All eruption styles exhibit a low-temperature mode at ~300 °C; lava fountains and 'a' ā flows also exhibit a higher-temperature mode at ~700 °C. The observed differences between the temperatures are consistent with the contrasting rates at which the lava surfaces are thermally renewed. Eruption styles that allow persistent and pervasive thermal renewal of the lava surface (e.g., fractured crusts on channel-fed 'a' ā flows) exhibit a bimodal temperature distribution; eruption styles that do not (e.g., the continuous skin of pāhoehoe lavas) exhibit a single mode. We conclude that insights into composition and eruption style can only be gained remotely by analyzing a large spatio-temporal sample of data. This has implications for determining composition and eruption style at the Jovian moon Io, for which no in situ validation is available.

INTRODUCTION

The surface temperature distribution of an active lava body has been used to derive information regarding lava composition and is a necessary boundary condition for estimating the rate at which lavas cool. It can also provide information regarding the degree to which lava crusts are fractured or flow surfaces thermally renew (Crisp and Baloga, 1990). Lava cooling is an important input into lava flow simulation models, as it drives the calculated changes in viscosity and yield strength, which determine the predicted cooling-limited length (Harris and Rowland, 2001). Temporal variations in the temperature of fractures on the surface of active lava domes have been found to be an indicator of their over-pressurization and the propensity of dome-hosting volcanoes to erupt explosively (Oppenheimer et al., 1993a). On the Jovian moon Io, lava surface temperatures of between 1400 and 1700 °C (McEwen et al., 1998) retrieved from analysis of data acquired during the National Aeronautics and Space Administration's (NASA's) Galileo mission have been used to argue for the eruption of ultramafic lavas, a conclusion that has implications for the thermal state of the Ionian mantle.

Although remote sensing has long offered the potential to document the detailed surface temperature characteristics of active lavas (Rothery et al., 1988), this promise has not yet been fully realized. This is in part because the data available have been of insufficient spectroradiometric fidelity to accurately retrieve lava surface temperatures over the commonly observed range of lava eruption conditions (Wright and Flynn, 2003). In Wright et al. (2010), we showed how spectral radiance data acquired by an imaging spectrometer (the Hyperion sensor carried on NASA's Earth Observing–1 [EO-1] spacecraft) can be used to quantify the surface temperature characteristics of active lavas, due to the fact that Hyperion provides unsaturated radiance data for all points on the active lava surface.

The objective of this work is to establish how the surface temperature distributions of terrestrial lavas vary as a function of eruption style and lava composition. This has been achieved by analyzing 61 hyperspectral remote sensing data sets covering the full range of common eruptive styles, including mafic lava fountains, lava flows (both 'a'ā and pāhoehoe types), and lava lakes, in addition to lava domes of intermediate and felsic composition. The images were acquired over 13 volcanoes, such that the provenance of the thermal emission data is well known with respect to the lava composition and eruption style that produced it.

METHOD

Hyperion acquires spectral radiance data in 242 wavebands between 0.4 and 2.5 μm at a spectral resolution of 10 nm and a spatial resolution of 30 m. The spectral radiance (L_λ) emitted from a lava surface can be written as:

$$L_\lambda = \sum_{i=1}^{n} f_i L(\lambda, T_i), \qquad (1)$$

where T_i is the temperature of the ith component and f_i is the fraction of the sensor's instantaneous field of view that it occupies. For any pixel, although some wavebands may saturate at longer wavelengths, useable radiance data can be found at increasingly shorter wavelengths. Saturated wavebands were excluded, and the remaining spectral measurements were corrected for the nonunitary graybody emissivity of the lava (basalt 0.95, Oppenheimer et al., 1993b; andesite 0.95, Oppenheimer et al., 1993a; dacite 0.82, Harris et al., 2002) and absorption of the surface-leaving radiance by the atmosphere (estimated using the MOD-TRAN [http://modtran.org/] radiative transfer code, assuming an appropriate atmosphere, season, and altitude for each volcano). Rothery et al. (1988) indicated that an uncertainty of ±0.2 in emissivity translates into only ±15 °C in pixel integrated temperatures, while the error introduced by the atmospheric correction is unlikely to exceed 5–10 °C. Nighttime data were used to avoid contamination of the emitted radiance by reflected sunlight. Pixels were identified as containing active lava if they exhibited spectral radiance >5 W m⁻² sr⁻¹ μm⁻¹ at 2.24 μm.

The best-fit solution of Equation 1 to each spectral radiance spectrum was then obtained, to yield a T_i-f_i solution for each image pixel, using the Levenberg-Marquardt method. T_i was allowed to float between limits of 100 °C (the theoretical lower sensitivity limit of Hyperion) and 1200 °C (beyond the basalt liquidus), while f_i was allowed to float between values of 0 and 1. The sum of the f_i values was constrained to not exceed one, but could (and usually did) sum to less than one, the remainder of the pixel being too cool to radiate significantly at these wavelengths. Wright et al. (2010) found that most solutions converged when $i = 2$ or 3. The solution with the lowest root mean square error was retained.

We analyzed 61 Hyperion images to quantify the surface temperature distributions of the lavas they contained. This group included 10 images of 'a'ā lava flows (Mount Etna, Sicily;

*E-mail: wright@higp.hawaii.edu.
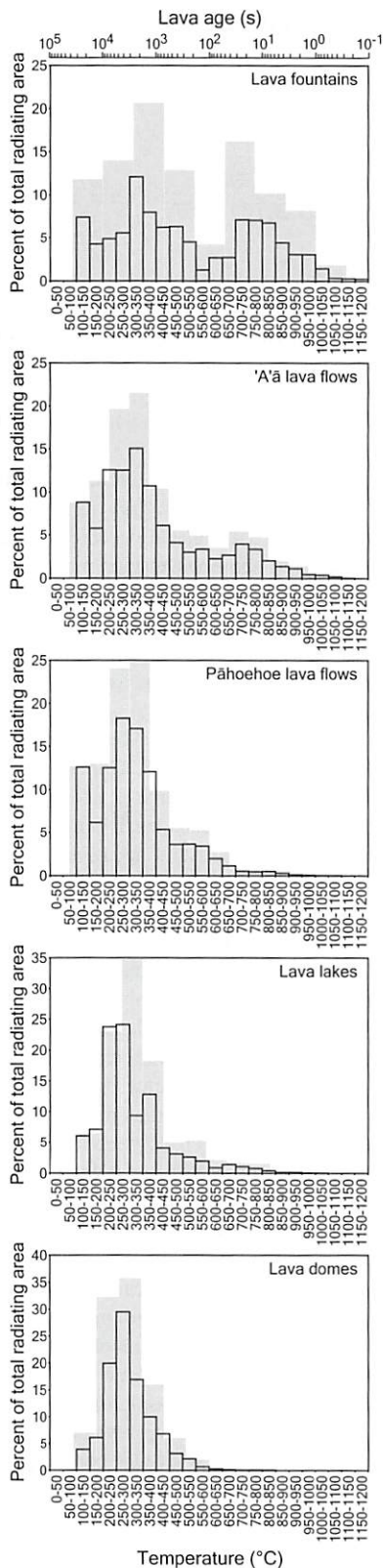
Figure 1. Histograms of lava surface temperature derived from NASA Hyperion imaging spectrometer data. Black-lined columns show data binned using arbitrary 50 °C intervals. Gray columns show same data rebinned. Upper abscissa shows time–surface temperature relationship determined by Keszthelyi et al. (2003) for cooling pāhoehoe lavas.

Mount Nyamuragira, Democratic Republic of Congo), 10 images of pāhoehoe flows (Kālauea, Hawai'i), 20 images of lava lakes (Erta 'Ale, Ethiopia; Mount Erebus, Antarctica; Mount Nyiragongo, Democratic Republic of Congo) and 20 images of lava domes (Mount St. Helens, United States; Chaitén, Chile; Santiaguito, Guatemala; Soufrière Hills, Montserrat; Shiveluch, Russia; Popocatépetl, Mexico). Due to the rarity of lava fountains, only one image of this eruption style, acquired during the during the Fimmvörðuháls phase of the 2010 eruption of Eyjafjallajökull (Iceland), was used. As such, fountains are underrepresented in the data set (128 pixels) when compared to 'a'ā flows (3771 pixels), pāhoehoe flows (2048 pixels), lava lakes (962 pixels), and lava domes (957 pixels).

RESULTS AND DISCUSSION

Figure 1 shows the T_i and f_i results obtained for each lava eruption style. Here, the area within each pixel occupied by lava at a given temperature has been calculated on a pixel-by-pixel basis (i.e., the sum of $f_i \times$ pixel area, for each T_i), for all images within a given eruption class (e.g., for all 2048 pāhoehoe pixels). The amount of lava at each temperature has then been expressed as the percentage of the total area of lava radiating at all temperatures (i.e., the area radiating at all values of T_i) within each class. The absence of lava with a temperature <~100 °C is an artifact resulting from the fact that the Hyperion instrument is insensitive to surfaces below this temperature.

## CONSTRAINING LAVA COMPOSITION FROM REMOTELY SENSED TEMPERATURE DATA

Lava eruption temperature varies systematically with composition; felsic and intermediate lavas typically erupt at temperatures of as much as a few hundred degrees below mafic lavas (Griffiths, 2000). Therefore, maximum lava surface temperature could be used as a proxy for determining composition remotely. The maximum temperatures derived from Hyperion indicate that this may not be so straightforward. Figure 2 shows the highest

Figure 2. Upper tenth percentile of temperatures retrieved from NASA Hyperion imaging spectrometer for each lava eruption style.

10% of temperatures calculated for each eruption style. For the pāhoehoe data as a whole, the 23 highest temperatures retrieved were between 1150 and 1199 °C. The latter is ~30 °C above the experimentally derived basaltic liquidus. During the 1984 eruption of Mauna Loa (Hawai'i), no temperatures in excess of 1150 °C were determined via any method (Lipman and Banks, 1987). Witter and Harris (2007) recorded lava surface temperatures at Kālauea no greater than 1164 °C. Thus, it appears that the maximum Hyperion-derived temperatures for the pāhoehoe lavas are slightly too high.

Similar reasoning suggests that the maximum Hyperion-derived temperature for 'a'ā (1178 °C) is also too high. For the dome observations, the maximum temperature was 1136 °C. The eruption temperatures of evolved lavas are typically lower than basalt by 350 °C (rhyolite), 250 °C (dacite), and 100 °C (andesite; Spera, 2000). The highest resolved temperature of 1073 °C at Chaitén appears to be too high for rhyolite. Only the maximum temperature determined for the lava fountains (1195 °C) does not exceed that expected on the basis of field observations, as Richter and Murata (1966) reported a temperature of 1190 °C for fountains at Kālauea. Our results show that any individual temperature retrieved from any individual pixel spectrum cannot be relied upon as a proxy for lava eruption temperature (and hence composition), as temperatures retrieved from analysis of mafic and intermediate and felsic lavas (1) exceed published maxima, and (2) overlap each other.

Although the radiance to temperature inversion results in uncertainty for individual pixels, leveraging the large amount of data available reveals significant differences in maximum temperature between mafic lavas and the intermediate and felsic lavas on a statistical basis. Excluding the highest 1% of the temperatures illustrated in Figure 2 yields revised maxima (99th percentile; T_{high}) of 1172 °C for the lava fountains, 1112 °C for the 'a'ā lavas, 1127 °C for the pāhoehoe lavas, 1126 °C for the lake lakes, and 940 °C for the lava domes. All are within the range of published observations, with T_{high} for the mafic lavas ~175–200 °C higher than that for the intermediate and felsic lavas, consistent with often quoted differences in eruption temperature between these compositions.

To determine if the temperatures shown in Figure 2 are statistically different from each other (i.e., values between the 90th and 99th percentile; T_{90-99}), an analysis of variance has been performed. For lava fountains, T_{90-99} with associated standard error is 1127 ± 6 °C. The corresponding T_{90-99} for 'a'ā flows is 1063 °C ± 1 °C, for pāhoehoe flows 1049 ± 1 °C, for lava lakes 1024 ± 2 °C, and for lava domes 855 ± 2 °C. Errors are 95% Bonferroni-Dunn confidence intervals (Sheskin, 1997). Based on
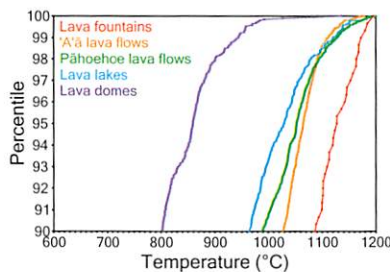
this analysis, domes have the lowest T_{90-99}, and lava fountains exhibit the highest. Clearly, factors such as surface texture and emplacement process strongly influence the surface temperature distributions of active lavas in addition to composition. However, when considering only the highest temperatures we retrieve from the remotely sensed data (i.e., the upper tail of the distribution), there is a statistically significant difference between the intermediate and felsic lavas and the mafic lavas.

CONSTRAINING LAVA ERUPTION STYLE FROM REMOTELY SENSED TEMPERATURE DATA

All of the distributions in Figure 1 contain a low-temperature mode, at ~200–400 °C. The amount of lava within this temperature range (as a percentage of total active lava area) increases in the order: lava fountains, 'a'ā flows, pāhoehoe flows, lava lakes, and lava domes. Fountains and 'a'ā flows exhibit a distinct high temperature mode (more pronounced in the former) at a temperature of ~700–900 °C. To assess whether the structure apparent in Figure 1 is an artifact of the arbitrary binning process, the data were rebinned (Fig. 1) using data-based binning guidelines (Sturges, 1926; Doane, 1976). The number of bins is primarily a function of the number of variates (Sturges, 1926). The lava lake and pāhoehoe lava flow data are sufficiently skewed that one additional bin has been included (Doane, 1976). Rebinning the fountain and 'a'ā flow data does not remove the high-temperature mode, and these peaks appear to be real components of the data. Pāhoehoe flows, lava lakes, and domes show no evidence for a second high temperature lava component.

Whereas differences in T_{high} correlate with gross differences in lava composition, the differences in modality and kurtosis can be most simply explained in terms of the average age of the surface of the lava bodies produced by each of these different eruption styles, and how that in turn depends on the temporal persistence and spatial pervasiveness of processes that serve to fracture cold crust, or otherwise thermally renew the lava surface. The upper abscissa of Figure 1 plots the time-lava surface temperature relationship derived by Keszthelyi et al. (2003) from in situ measurements of the cooling of pāhoehoe lobes (extrapolated to 0–1200 °C). For purposes of illustration (and assuming that silicate melts cool at approximately the same rate regardless of morphology), a surface temperature of 200–400 °C corresponds to lava older than 0.5–3 h. Conversely, lava with a temperature of ~650–750 °C can only have been exposed to the atmosphere within tens of seconds of spacecraft overpass.

All styles exhibit a low temperature mode, as for all there will be some lava within the image pixel that is tens of minutes to hours old. Only the 'a'ā flows and fountains expose a significant amount of lava to the sensor that is of the order of tens of seconds old. Given the rapid rate at which lava cools when at a temperature of ~700 °C (within ~100 s of emplacement the lava will be below 600 °C; within ~500 s, below 500 °C; Fig. 1), this indicates that the thermal renewal of the lava's upper surface for these features is pervasive in space (to affect many pixels) and persistent in time (to have been sampled by the orbital sensor, for which the integration time per measurement is measured in milliseconds). This is consistent with differences in the style of emplacement for those lava types depicted in Figure 1.

For lava fountains, high temperatures are maintained over extended periods of time due to high flux rates and the small range of angles over which clasts are ejected from the vent, which produces optically thick fountains that retard heat loss (Head and Wilson, 1986). This ensures that ample young, hot lava will be exposed to an orbiting satellite, explaining the high temperature mode in the data (Fig. 1). The lava cools rapidly once it strikes the ground to be emplaced as a combination of spatter and lava flows, producing the lower-temperature mode. However, at the planimetric scale of the feature, the ratio of young, hot lava, to older, cooler lava is relatively high, resulting in distinct bimodality.

For channel-fed 'a'ā flows, motion of the core causes fracturing of the overlying crust (Crisp and Baloga, 1990), and hot material from the interior is continually exposed to a spacecraft via cracks in this crust. The material in the cracks cools to become crust within seconds to tens of seconds. However, while the flow is active the process operates continuously to ensure that some young, hot lava is continuously exposed at the surface. Furthermore, fracturing of the crust is pervasive over the surface of the moving flow. This combination of temporal persistence and spatial pervasiveness explains the higher-temperature mode in the 'a'ā flow data. The high-temperature mode of the 'a'ā data is less pronounced than for the fountains (i.e., at the scale of the feature, the ratio of young lava to older lava is lower). This is consistent with the commonly observed difference in the preponderance of incandescent lava apparent between the two eruption styles.

In contrast, the derived surface temperatures for pāhoehoe flows show no evidence of a high temperature mode. Pāhoehoe lavas are characterized by a continuous skin, in contrast to 'a'ā flows, which have a discontinuous surface crust (Rowland and Walker, 1990). This skin reduces cooling and insulates the lava core. Although incandescence is observed in the field, it is usually confined to the edges of lobes (or at points of breakout). Thus, although persistent in time, exposure of young, hot lava at the surface is not pervasive over the entire surface of a growing pāhoehoe flow or flow field. While high-temperature lava is resolved by Hyperion for pāhoehoe flows (evidenced by the tail in the distribution) it is of insufficient areal abundance within the pixel to produce a second mode in the temperature distribution.

The lava lake data are also unimodal. The crust on a lava lake is constantly disrupted, although the exposure of hot lava tends to be at the boundaries between large plates, rather than pervasive over the entire surface area of the lake. Fountaining at the lake surface, or overturning events, will cause an increase in the exposure of hot lava to the spacecraft, but the duration of these events is shorter than the repose times between them. Harris et al. (2005) estimated that periods of vigorous activity at Erta 'Ale last 1–3 h, while the intervening periods of sluggish activity last 1–10 h. A spacecraft that images a target once every two weeks and takes microseconds to make each measurement is more likely to sample a high-temperature mode corresponding to thermal renewal processes that are extensive and persistent ('a'ā flows and lava fountains) than those that are persistent but spatially limited (pāhoehoe flows) or episodic in time (lava lakes). The absence of a high-temperature mode for the lava domes is most simply explained by the fact that the lava is more viscous, and typically erupted at lower mass flux rates (Griffiths, 2000). Thermally renewing a lava surface is difficult under such circumstances, either in space or time.

CONCLUSIONS

Our results indicate that lava surface temperatures derived from hyperspectral remotely sensed radiance data can be used to provide information regarding lava composition and eruption style, in the absence of ancillary information. However, this appears to be contingent on having sufficient data to compile robust lava surface temperature distributions. Using satellite data acquired for terrestrial lavas of known composition, we find that analysis of any individual pixel's spectrum can yield a maximum temperature that is unreasonably high. However, with a sufficiently large sample, extreme values can be ignored, and the remaining data indicate a statistically significant difference in the highest temperature retrieved for mafic lavas and intermediate and felsic lavas. In light of this result, future missions to the Jovian moon Io should aim to collect as many data as possible if eruption temperatures, and the composition of Ionian lavas, are to be determined on the basis of remotely sensed temperature data: our experience with terrestrial targets of known composition indicates that maximum derived temperature from spectral radiance data is not a

reliable proxy, even for gross differences in lava composition, if data are scanty.

The temperature distributions correlate with differences in eruption style. Bimodal distributions are characteristic of styles that result in temporally persistent and spatially pervasive exposure of young, hot lava to the spacecraft (lava fountains and channel-fed 'a'ā flows). Styles for which such thermal renewal of the lava surface is either spatially limited (pāhoehoe flows), temporally episodic (lava lakes), or both (lava domes), lack a second high-temperature mode and are instead characterized by log-normal distributions. The compositionally more evolved domes may be discriminated from the latter due to a statistically significant difference in the highest resolved temperature. However, on the basis of surface temperature distribution alone, pāhoehoe flows and lava lakes are very similar to each other. This has implications for Io volcanologists, for whom debate continues as to whether Loki volcano hosts a persistent (but, at 200 km in diameter, enormous) lava lake, or simply caldera-confined pāhoehoe lava flows (Gregg and Lopes, 2008).

Adequate temporal sampling is also necessary if differences in eruption style are to be resolved. As soon as a channel-fed 'a'ā flow stops moving, the surface of the flow is no longer thermally renewed, the second high-temperature mode will dissipate, and the temperature distribution will tend toward that of the log-normal pāhoehoe lavas (Wright et al., 2010, their Fig. 7). Equally, a single observation of a lava lake undergoing an overturning event may yield a temperature distribution with a second high temperature mode, thus resembling a fountain.

REFERENCES CITED
Crisp, J.A., and Baloga, S.M., 1990, A model for lava flows with two thermal components: Journal of Geophysical Research, v. 95, p. 1255–1270, doi:10.1029/JB095iB02p01255.

Doane, D.P., 1976, Aesthetic frequency classifications: American Statistician, v. 30, p. 181–183, doi:10.2307/2683757.

Gregg, T.K.P., and Lopes, R.M., 2008, Lava lakes on Io: New perspectives from modeling: Icarus, v. 194, p. 166–172, doi:10.1016/j/Icarus.2007.08.042.

Griffiths, R.W., 2000, The dynamics of lava flows: Annual Review of Fluid Mechanics, v. 32, p. 477–518, doi:10.1146/annurev.fluid.32.1.477.

Harris, A.J.L., and Rowland, S.K., 2001, FLOWGO: A kinematic thermo-rheological model for lava flowing in a channel: Bulletin of Volcanology, v. 63, p. 20–44, doi:10.1007/s004450000120.

Harris, A.J.L., Flynn, L.P., Matias, O., and Rose, W.I., 2002, The thermal stealth flows of Santiaguito dome, Guatemala: Implications for the cooling and emplacement of dacitic block-lava flows: Geological Society of America Bulletin, v. 114, p. 533–546, doi:10.1130/0016-7606(2002)114<0533:TTSFOS>2.0.CO;2.

Harris, A.J.L., Carniel, R., and Jones, J., 2005, Identification of variable convective regimes at Erta Ale lava lake: Journal of Volcanology and Geothermal Research, v. 142, p. 207–223, doi:10.1016/j.jvolgeores.2004.11.011.

Head, J.W., and Wilson, L., 1986, Volcanic processes and landforms on Venus: Theory, predictions, and observations: Journal of Geophysical Research, v. 91, p. 9407–9446, doi:10.1029/JB091iB09p09407.

Keszthelyi, L., Harris, A.J.L., and Dehn, J., 2003, Observations of the effect of wind on the cooling of active lava flows: Geophysical Research Letters, v. 30, 1989, doi:10.1029/2003GL017994.

Lipman, P.W., and Banks, N.G., 1987, Aa flow dynamics, Mauna Loa 1984, in Decker, R., et al., eds., Volcanism in Hawaii: U.S. Geological Survey Professional Paper 1350, p. 1527–1567.

McEwen, A.S., and 14 others, 1998, High-temperature silicate volcanism on Jupiter's moon Io: Science, v. 281, p. 87–90, doi:10.1126/science.281.5373.87.

Oppenheimer, C., Francis, P.W., Rothery, D.A., Carlton, R.W.T., and Glaze, L.S., 1993a, Infrared image analysis of volcanic thermal features: Lascar Volcano, Chile, 1984–1992: Journal of Geophysical Research, v. 98, p. 4269–4286, doi:10.1029/92JB02134.

Oppenheimer, C., Rothery, D.A., Pieri, D.C., Abrams, M.J., and Carrere, V., 1993b, Analysis of Airborne Visible/Infrared Imaging Spectrometer (AVIRIS) data of volcanic hot spots: International Journal of Remote Sensing, v. 14, p. 2919–2934, doi:10.1080/01431169308904411.

Richter, D.H., and Murata, K.J., 1966, Petrography of the lavas of the 1959–60 eruption of Kilauea volcano, Hawaii: U.S. Geological Survey Professional Paper 537-D, 12 p.

Rothery, D.A., Francis, P.W., and Wood, C.A., 1988, Volcano monitoring using short wavelength infrared satellite data: Journal of Geophysical Research, v. 93, p. 7993–8008, doi:10.1029/JB093iB07p0799.

Rowland, S.K., and Walker, G.P.L., 1990, Pahoehoe and aa in Hawaii: Volumetric flow rate controls the lava structure: Bulletin of Volcanology, v. 52, p. 615–628, doi:10.1007/BF00301212.

Sheskin, D.J., 1997, Handbook of parametric and nonparametric statistical procedures: New York, CRC Press, 719 p.

Spera, F.J., 2000, Physical properties of magmas, in Sigurdsson, H., et al., eds., Encyclopedia of volcanoes: San Diego, California, Academic Press, p. 171–190.

Sturges, H.A., 1926, The choice of a class interval: American Statistical Association Journal, v. 21, p. 65–66.

Witter, J.B., and Harris, A.J.L., 2007, Field measurements of heat loss from skylights and lava tube systems: Journal of Geophysical Research, v. 112, B01203, doi:10.1029/2005JB003800.

Wright, R., and Flynn, L.P., 2003, On the retrieval of lava flow surface temperatures from infrared satellite data: Geology, v. 31, p. 893–896, doi:10.1130/G19645.1.

Wright, R., Garbeil, H., and Davies, A.G., 2010, Cooling rate of some active lavas determined using an orbital imaging spectrometer: Journal of Geophysical Research, v. 115, B06205, doi:10.1029/2009JB006536.